the plant journal

SEB SOCIETY FOR EXPERIMENTAL BIOLOGY

The Plant Journal (2022) **112,** 1159–1175 doi: 10.1111/tpj.16002

Chrysanthemum MAF2 regulates flowering by repressing gibberellin biosynthesis in response to low temperature

Jing Lyu[1,2,†], Palinuer Aiwaili[1,2,†], Zhaoyu Gu[2], Yanjie Xu[2], Yunhan Zhang[2], Zhiling Wang[2], Hongfeng Huang[2], Ruihong Zeng[2], Chao Ma[1,2], Junping Gao[1,2], Xin Zhao[1,3,*] and Bo Hong[1,2,*]

[1]*State Key Laboratory for Agrobiotechnology, College of Biological Sciences, China Agricultural University, Beijing 100193, China,*

[2]*Beijing Key Laboratory of Development and Quality Control of Ornamental Crops, Department of Ornamental Horticulture, China Agricultural University, Beijing 100193, China, and*

[3]*State Key Laboratory of Plant Physiology and Biochemistry, College of Biological Sciences, China Agricultural University, Beijing 100193, China*

Received 24 May 2022; revised 26 September 2022; accepted 7 October 2022; published online 10 October 2022.
*For correspondence (e-mail zhaoxin5691@cau.edu.cn; hongbo1203@cau.edu.cn).
†These authors contributed equally to this work.

SUMMARY

Chrysanthemum (*Chrysanthemum morifolium*) is well known as a photoperiod-sensitive flowering plant. However, it has also evolved into a temperature-sensitive ecotype. Low temperature can promote the floral transition of the temperature-sensitive ecotype, but little is known about the underlying molecular mechanisms. Here, we identified *MADS AFFECTING FLOWERING 2* (*CmMAF2*), a putative MADS-box gene, which induces floral transition in response to low temperatures independent of day length conditions in this ecotype. CmMAF2 was shown to bind to the promoter of the GA biosynthesis gene *CmGA20ox1* and to directly regulate the biosynthesis of bioactive GA_1 and GA_4. The elevated bioactive GA levels activated *LEAFY* (*CmLFY*) expression, ultimately initiating floral transition. In addition, *CmMAF2* expression in response to low temperatures was directly activated by CmC3H1, a CCCH-type zinc-finger protein upstream. In summary, our results reveal that the CmC3H1–CmMAF2 module regulates flowering time in response to low temperatures by regulating GA biosynthesis in the temperature-sensitive chrysanthemum ecotype.

Keywords: *Chrysanthemum morifolium*, low-temperature flowering, *CmMAF2*, *CmC3H1*, GA biosynthesis.

INTRODUCTION

Adaptation of flowering plants to environmental conditions to ensure appropriate flowering time is critical for reproductive success (Amasino, 2009). To this end, angiosperms have evolved diverse strategies that vary depending on whether they are exposed to external stimuli (photoperiod and vernalization) or endogenous cues (autonomous, gibberellins [GAs], and aging), which are interconnected and form a complex network that regulates flowering (Song et al., 2013; Srikanth & Schmid, 2011). For vernalization-requiring plants, prolonged exposure to low temperatures can promote their flowering ability (Ream et al., 2012), and some of the mechanisms underlying low temperature-induced flowering have been elucidated in the experimental model plant *Arabidopsis thaliana* (Xu & Chong, 2018). In winter-annual *A. thaliana*, *FLOWERING LOCUS C* (*FLC*) encodes a MADS-box transcription factor that acts as a core floral repressor (Amasino, 2004; Michaels & Amasino, 1999). There are three phases of *FLC* expression: a high level of *FLC* expression prior to vernalization, silencing of *FLC* expression during vernalization, and stable maintenance of *FLC* silencing upon returning to warmer conditions. It has been shown that flowering competence is acquired through a direct upregulation of *FLOWERING LOCUS T* (*FT*) (Gu et al., 2013; Whittaker & Dean, 2017). It is also known that in biennial winter varieties of wheat (*Triticum aestivum*) and barley (*Hordeum vulgare*), *VERNALIZATION 1* (*VRN1*), a homolog of *A. thaliana APETALA 1*, is the key floral activator during vernalization (Xu & Chong, 2018) and that in perennial *Arabis alpina* (a relative of the annual *A. thaliana*), *PERPETUAL FLOWERING1* (*PEP1*) confers the vernalization requirement (Wang et al., 2009).

MADS AFFECTING FLOWERING 2 (*MAF2*) is a member of the MADS-box transcription factor gene family in Arabidopsis, which has five members (*MAF1–5*). These

genes are close homologs of *FLC* and have also been shown to regulate flowering time in response to low temperatures (Gu et al., 2013; Ratcliffe et al., 2003). *MAF2* expression is less sensitive to vernalization than *FLC* and works either independently or downstream from FLC (Ratcliffe et al., 2003). Nevertheless, the intricate network by which MAF2 regulates flowering time remains unclear.

The Asteraceae family is regarded as the most diverse family of flowering plants (Barreda et al., 2015). Chrysanthemum (*Chrysanthemum morifolium*) is a perennial herbaceous member of Asteraceae, whose floral induction mainly depends on the photoperiodic pathway (Higuchi et al., 2013). Hence, chrysanthemum has evolved several different ecotypes due to the differences in critical day length for flowering (Kawata, 1987). However, low temperature also has major effects on the flowering of different chrysanthemum ecotypes. In particular, there is a low temperature-sensitive ecotype whose floral induction requires low-temperature exposure, which is also referred to as vernalization (Harada & Nitsch, 1959; Hisamatsu et al., 2017; Schwabe, 1950; Schwabe, 1954). Indeed, several chrysanthemum varieties form a rosette without low-temperature treatments, indicating a typical vernalization requirement (Sumitomo et al., 2009). Nevertheless, it is still unknown how chrysanthemum regulates floral transition in response to low temperatures.

Genetic analyses have identified the plant hormone GA as having a prominent role in flowering time regulation. Among the GA compounds, only those that are bioactive, such as GA_1, GA_3, and GA_4, function in regulating floral transition (Binenbaum et al., 2018; Langridge, 1957; Mutasa-GÖttgens & Hedden, 2009; Song et al., 2013). In *A. thaliana*, the application of GAs rescues the flowering mutant phenotype under non-inductive short-day (SD) conditions (Langridge, 1957). Flower initiation in *A. thaliana* under non-inductive SD conditions depends on the biosynthesis of GA and on the regulation of the expression of the flower meristem identity gene *LEAFY* (*LFY*) (Eriksson et al., 2006). Studies have shown that three major oxidase genes regulate GA biosynthesis and inactivation: *GA20-oxidase* (*GA20ox*), *GA3-oxidase* (*GA3ox*), and *GA2-oxidase* (*GA2ox*) (Lee & Zeevaart, 2007; Rieu et al., 2008). Overexpression of *GA20ox* promotes shoot elongation and early flowering in *A. thaliana* (Lee & Zeevaart, 2007; Rieu et al., 2008), and similarly, in SD chrysanthemum, GAs can promote flowering under non-inductive long-day (LD) conditions (King, 2012; Pharis, 1972; Yang et al., 2014).

Studies in different species have established a physiological connection between low-temperature conditions and GA metabolism. In the Brassicaceae species field pennycress (*Thlaspi arvense* L.), vernalization was found to affect GA metabolism by increasing the levels of the GA precursor kaurenoic acid (Hazebroek et al., 1993). Furthermore, in winter canola (*Brassica napus*), the abundance of active GA_1 and GA_3 increased following vernalization treatment (Zanewich & Rood, 1995). Finally, in lisianthus (*Eustoma grandiflorum*), levels of the GA precursor *ent*-kaurene were shown to be increased by low-temperature exposure, leading to higher endogenous GA_1 levels (Hisamatsu et al., 2004). However, the molecular mechanisms underlying the connections between low temperature and GA metabolism remain largely unknown.

Members of the Cys_3His-type zinc-finger protein superfamily are involved in many aspects of plant growth and development (Bogamuwa & Jang, 2014). In Arabidopsis, TZF1 (AtC3H23), a Cys_3His-type family member, can affect plant growth and stress responses (Lin et al., 2011). AtTZF2 (AtOZF1/AtC3H20) and AtTZF3 (AtOZF2/AtC3H49) are involved in ABA, jasmonate, and oxidative stress responses (Huang et al., 2011; Huang et al., 2012; Lee et al., 2012). However, little is known about the roles of Cys_3His-type zinc finger proteins in regulating flowering time.

In the current study, we report that low temperature is a key environmental factor in inducing the floral transition of a temperature-sensitive chrysanthemum ecotype. We present evidence for a novel mechanism of low-temperature response in chrysanthemum in which the CmC3H1–CmMAF2 module contributes to the induction of flowering. Our results reveal that in response to low temperatures, *CmMAF2* expression was directly induced by CmC3H1, and CmMAF2 directly targeted *CmGA20ox1*, elevating bioactive GA levels and in turn activating *CmLFY* expression, ultimately resulting in flowering. Our discovery of this mechanism will contribute to the development of flowering technologies and the annual production of different chrysanthemum ecotypes.

RESULTS

Low temperatures induce the capacity for flowering

To investigate the impact of extended low-temperature periods on physiological mechanisms that govern flowering in chrysanthemum, we used a cultivar that is sensitive to low temperatures (*C. morifolium* cv. Summer Yellow). As shown in Figure 1, under LD conditions, plant growth was severely inhibited by 1–5 weeks of low-temperature treatment (LT1–LT5), and the growth rate increased after returning to normal temperatures for 1–5 weeks (recovery phase LT5 + N1 to LT5 + N5). The treated plants reached the same height as the control plants after returning to normal temperatures for 5 weeks (LT5 + N5) (Figure 1a,b). We then tested the effects of low temperatures on growth under SD conditions. Control plants grew slowly (C8–C13), while plants exposed to low temperature for 8 weeks showed rapid growth and were significantly taller than the control, ultimately reaching the proper height (LT8 + N5) (Figure S1).

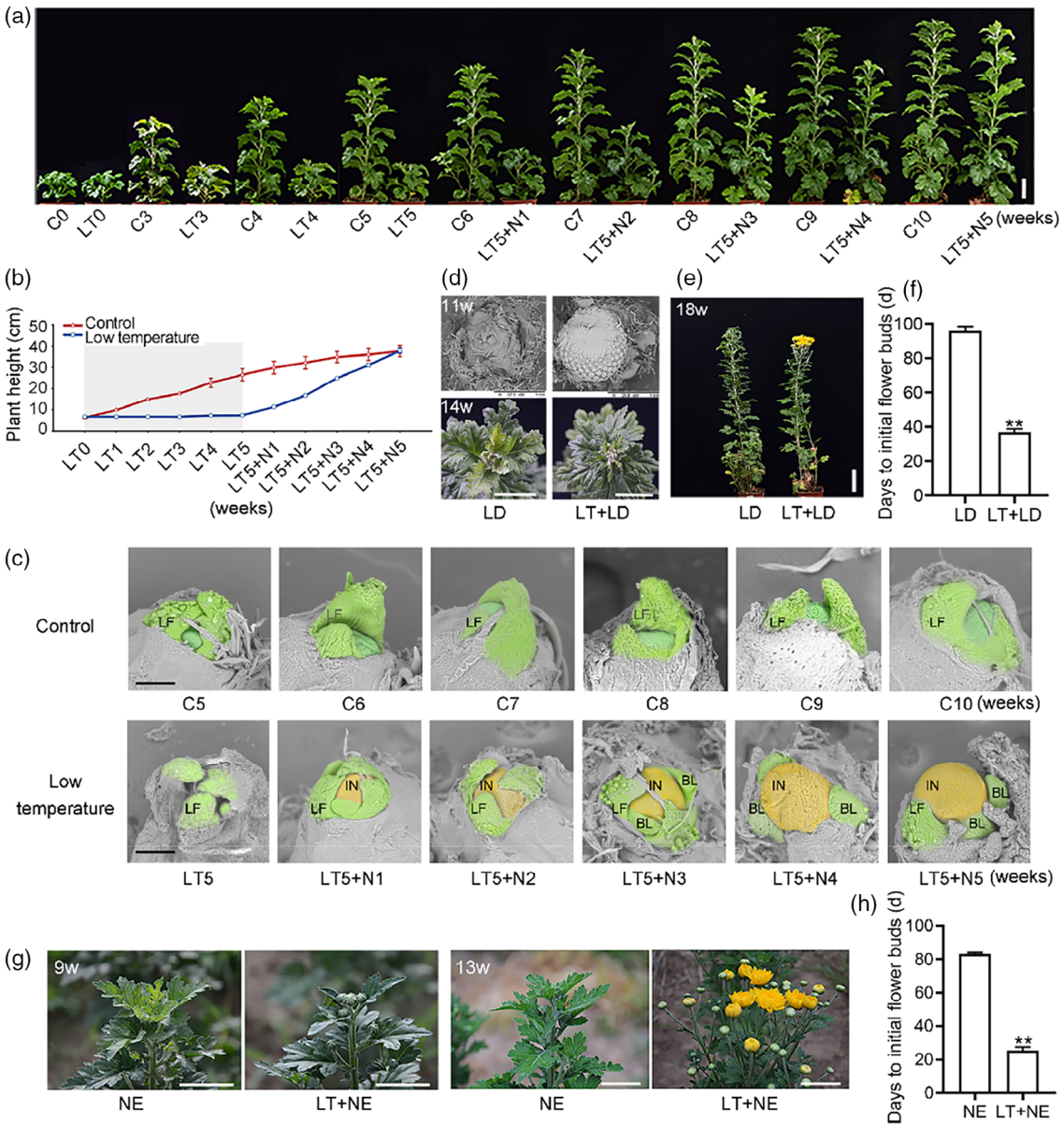

Figure 1. Chrysanthemum flowering in response to low temperature. (a) Plants were grown for 5 weeks at low temperature (LT1–5) and then returned to normal temperature for recovery (LT5 + N1–N5). Control plants (C1–10) were grown under normal temperature and LD conditions. The phenotypes were observed daily. Scale bars, 5 cm. (b) Plant heights after 5 weeks of growth at low temperature (LT1–5) and 1–5 weeks after returning to normal temperature (LT5 + N1–N5). (c) Scanning electron microscopy images of apex development in plants grown at low temperatures for 5 weeks or at normal temperatures under LD conditions. C5–10, 5–10-week control; LT5, 5-week low-temperature treatment; LT5 + N1–5, 1–5 weeks after returning to normal temperature; LF, leaf primordium; IN, involucre; BL, bract leaf primordium. Scale bars, 200 μm. (d) Scanning electron microscopy images of inflorescence and flower bud morphology in plants treated for 5 weeks with low temperature (LT + LD) or without low temperature (LD) after 11 weeks and 14 weeks under LD conditions. Scale bars, 5 cm. (e) Blooming phenotype in plants treated for 5 weeks with low temperature (LT5) or without low temperature (LD) after 18 weeks under LD conditions. Scale bars, 5 cm. (f) Days until initial flower bud emergence in plants treated for 5 weeks with low temperature or without low temperature. (g) The phenotype of plants treated for 5 weeks with low temperature (LT + natural environment [NE]) or without low temperature (NE) after 9 weeks and 13 weeks in the field and photographed on 6 June and 30 June, respectively (Beijing, China). Scale bars, 5 cm. (h) Days until initial flower bud emergence in plants treated for 5 weeks with low temperature (LT + NE) or without low temperature (NE). The results are the means of five biological replicates with standard deviations. Asterisks indicate statistically significant differences (Student's *t*-test, $^{**}P < 0.01$).

Next, we determined the flowering time in response to low temperatures under different day lengths. Under LD conditions, microscopic observation showed that the apical meristem of plants treated with low temperatures began to exhibit hypertrophy at LT5 + N1, entered the early stage of involucral primordium at LT5 + N3, and formed the involucral primordium at LT5 + N5, while the control plants (C5–C10) remained in the vegetative stage (Figure 1c). The time to floret primordium formation, the development of an apical inflorescence, and flower

Table 1 Differentially expressed genes related to flowering time at 5 weeks at low temperature (LT5), and at 1 and 5 weeks after returning to normal temperature (LT5 + N1, LT5 + N5)

Gene	Annotation	RPKM (C5)	RPKM (LT5)	RPKM (LT5 + N1)	RPKM (LT5 + N5)
Vernalization pathway					
Cluster-17868.118397	*CmMAF2*	10.62 ± 1.02bc	24.04 ± 3.34a	15.49 ± 2.97b	8.83 ± 0.52c
Gibberellin pathway					
Cluster-17868.212239	*GA20ox1*	1.17 ± 0.14a	0.27 ± 0.16b	1.22 ± 0.21a	0.34 ± 0.17b
Cluster-17868.71469	*GA2ox*	0.80 ± 0.30b	4.02 ± 0.50a	1.10 ± 0.33b	1.37 ± 0.15b
Cluster-17868.234688	*GA3ox*	3.00 ± 0.85b	12.50 ± 4.98a	1.81 ± 0.53b	0.41 ± 0.21b
Cluster-17868.223832	*GID1c*	2.91 ± 0.74c	8.50 ± 0.25a	6.29 ± 1.22b	1.57 ± 0.36c
Cluster-17868.139458	*GAI-like*	22.47 ± 1.75b	9.44 ± 1.00c	44.58 ± 12.78a	41.44 ± 0.92a
Cluster-17868.147300	*RGA*	31.17 ± 1.11a	13.18 ± 1.09b	30.16 ± 1.29a	31.41 ± 1.05a
Flowering integrator					
Cluster-17868.27582	*AFT*	0.94 ± 0.03c	0.80 ± 0.28c	4.73 ± 0.40a	2.66 ± 0.42b
Cluster-17868.32465	*AFL2*	4.23 ± 0.96a	1.56 ± 0.22b	0.78 ± 0.40b	5.73 ± 0.93a
Cluster-17868.114531	*FDL1*	4.01 ± 1.32a	4.04 ± 0.14a	1.82 ± 0.52b	1.42 ± 0.07b
Cluster-17868.147733	*FDL2*	9.91 ± 0.16a	7.81 ± 0.91b	10.05 ± 0.85a	7.76 ± 0.77b
Cluster-17868.233356	*FTL2*	0.25 ± 0.01c	0.78 ± 0.07b	0.16 ± 0.04c	1.27 ± 0.06a
Cluster-17868.71935	*FTL3*	3.25 ± 0.08b	1.10 ± 0.13c	0.27 ± 0.08c	5.88 ± 1.10a

Three independent experiments were performed; '±' indicates standard deviation. Different letters indicate significant differences according to Duncan's multiple range test ($P < 0.05$).

blooming occurred significantly earlier after a 5-week low-temperature treatment at 11 weeks (LT5 + N6), 14 weeks (LT5 + N9), and 18 weeks (LT5 + N13) compared to non-treated plants (Figure 1d,e). There was also a statistically significant difference in initial flower bud formation (diameter = 2 mm). They were observed at 37 ± 1.7 days after transplanting in plants treated with low temperatures and at 96 ± 2.2 days after transplanting in non-treated control plants (Figure 1f). We then tested the effect of low temperatures on flowering in natural environments by transplanting plants that have been treated for LT5 to the field. We observed that floral buds appeared and bloomed significantly earlier in plants treated with low temperatures than control plants (Figure 1g,h). Under SD conditions, no flower buds were observed for 200 days on the control plants, while the emergence of initial flower buds was observed at 105 ± 5.0 days following an 8-week low-temperature treatment (Figure S1). These data indicate that low temperatures induce the capacity for flowering independent of the photoperiod.

Endogenous GA levels are associated with low temperature-induced flowering

We analyzed the RNA sequencing (RNA-seq) data from low temperature-treated and control plants in the floral transition phase. The results showed that GA pathway genes were differentially expressed (Table 1). To test this, we measured endogenous GA levels under low-temperature conditions and in the recovery phase. We observed that compared with C5, the low-temperature treatment LT5 caused a significant decrease in the abundance of bioactive GA_1, its precursor GA_{20}, and its metabolite GA_8. However, compared with C7, GA_1, GA_{20}, and GA_8 levels were higher at LT5 + N2 (Figure 2a). Similarly, the concentrations of bioactive GA_4 and its precursor GA_9 were significantly reduced in LT5 but were higher in LT5 + N2 plants (Figure 2a). Thus, growth inhibition due to low temperatures, combined with early flowering in the recovery phase, was correlated with the change in active GA levels.

We next verified the relationship between GA levels and low temperature during chrysanthemum flowering by applying exogenous GA. Under LD conditions, plant height significantly increased after application of 100 μM $GA_{4/7}$ compared to the control. In addition, the time to flowering was earlier in the plants treated with $GA_{4/7}$ and similar to that in plants treated with low temperatures for 5 weeks (Figure 2b–d).

Under SD conditions, an increase in plant height was observed in plants treated with 100 μM $GA_{4/7}$ or low temperature (Figure S2a,b). However, no flower buds appeared on the control plants by day 200 after transplanting, while 100 μM $GA_{4/7}$ and low temperature-treated plants had flower buds by day 137 ± 1.6 and 105 ± 5.0, respectively (Figure S2a–c). These results indicate that the effects of low temperature on flowering time are associated with GA biosynthesis.

CmMAF2 and *CmGA20ox1* expression is regulated by low temperatures

To elucidate the molecular mechanisms underlying floral induction in response to low temperatures in chrysanthemum, we identified differentially expressed genes at LT5, LT5 + N1, and LT5 + N5. We observed that the expression of a putative MADS-box gene (Cluster-17868.118397) was

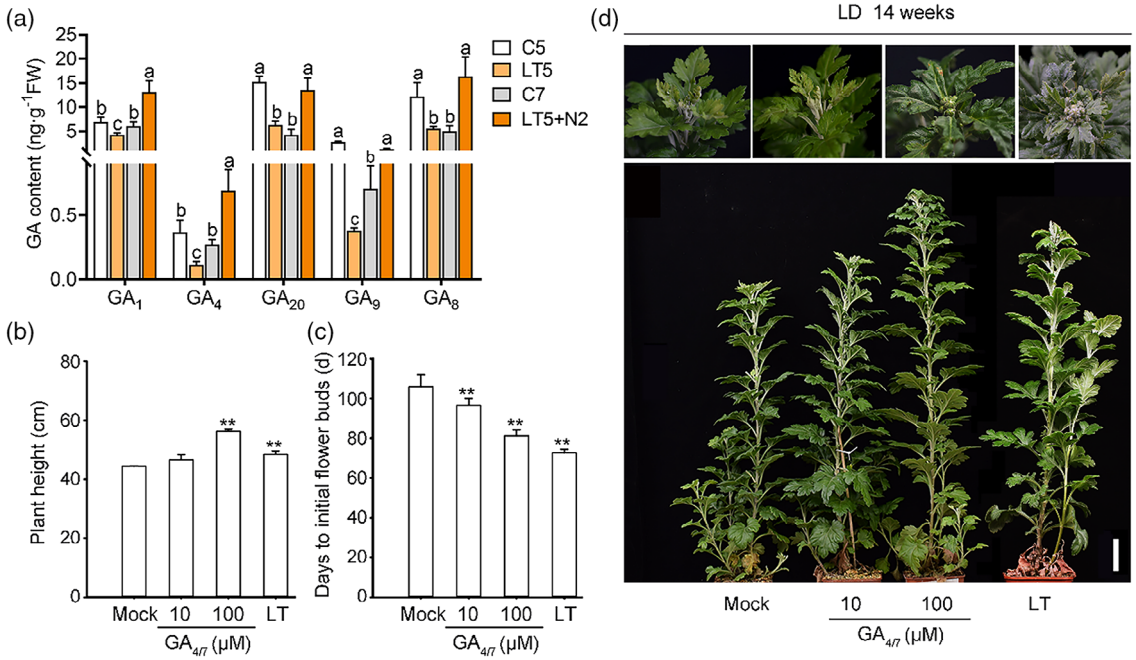

Figure 2. Effects of GA treatments on chrysanthemum flowering under LD conditions. (a) GA content in the shoot tips of plants at LT5 and at LT5 + N2. Plants grown for 5 or 7 weeks under normal temperature and LD conditions were used as controls (C5 and C7). (b) The effects of exogenous $GA_{4/7}$ treatment and 5-week low-temperature treatment (LT5) on plant height of 8-week-old chrysanthemum. GA was given twice per week for 2 months. (c) The effects of exogenous $GA_{4/7}$ treatments and 5-week low-temperature treatments (LT5) on initial flower bud appearance in control and treated plants. (d) Phenotypes of control and treated plants were observed after 14 weeks. The results are the means of three biological replicates with standard deviations. Asterisks indicate statistically significant differences (Student's *t*-test, $^{**}P < 0.01$). Different letters indicate significant differences according to Duncan's multiple range test ($P < 0.05$). Scale bars, 5 cm.

2.3-fold higher in LT5-treated plants compared with controls. Its expression in treated plants gradually decreased after returning to normal temperature (Table 1; Data S1). Amino acid sequence alignment showed that Cluster-17868.118397 had a high degree of sequence homology to *A. thaliana* MAF2, so this gene was re-named *CmMAF2* (Figure S3a,b). In addition, the expression of the GA biosynthesis gene *CmGA20ox1* (Cluster-17868.212239) decreased 4.3-fold in LT5-treated plants compared with controls, while its expression gradually increased after returning to normal temperatures (Table 1; Data S1).

We measured the mRNA expression levels of *CmMAF2* in leaves and shoot tips using quantitative real-time PCR (qRT-PCR) and found that both of them were upregulated during low-temperature treatments and down-regulated after returning to normal temperatures (Figure 3a,b). However, the expression of the GA biosynthesis gene *CmGA20ox1* showed a reverse trend, being repressed by the low-temperature treatment and increasing after returning to normal temperatures in both leaves and shoot tips (Figure 3c,d). This expression pattern was consistent with the results from an *in situ* hybridization analysis, showing that *CmGA20ox1* expression in apical meristems was lower under low-temperature conditions than under control conditions. *CmGA20ox1* expression was higher at LT + N1 (Figure 3e). Unlike *CmGA20ox1*, the expression of another *GA20ox* gene, *CmGA20ox2*, was slightly and continuously suppressed by low temperatures, and the expression did not recover after returning to normal temperatures (Figure S3c).

To understand the effects of low temperatures on flower initiation in chrysanthemum, we determined the expression levels of *CmFTL1*, *CmFTL2*, and *CmFTL3*, three *FT*-homologous genes, and *CmLFY*, a flower meristem identity gene. The results showed no significant differences in the expression of *CmFTL1–3* between low-temperature treatment and control plants in both leaves and shoot tips (Figure S2e–j). *CmLFY* expression in shoot tips was not significantly changed compared to the control during the low-temperature treatments, while *CmLFY* expression was significantly increased at 2 weeks after returning to normal temperatures, which is the time point for floral transition (Figure 3f). We also determined *CmLFY* expression levels during $GA_{4/7}$ and paclobutrazol (PAC) treatments, and the results showed that *CmLFY* expression was significantly induced by GA, while it was inhibited by PAC (Figure S2d). These data suggest that *CmGA20ox1* and *CmLFY* might participate in flowering regulation in low temperature-induced chrysanthemum ecotypes.

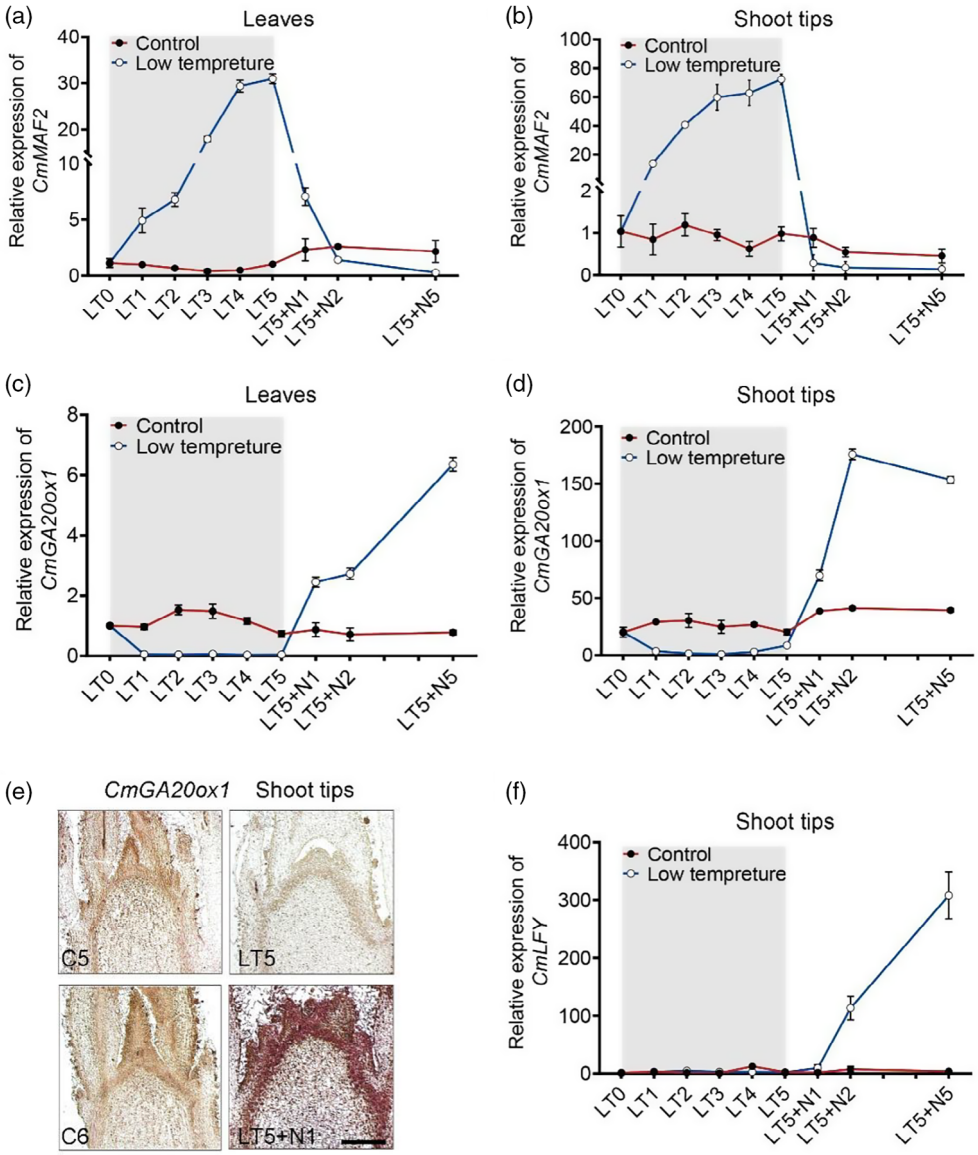

Figure 3. *CmMAF2*, *CmGA20ox1*, and *CmLFY* expression in response to low temperature (LT). (a,b) Expression of *CmMAF2* was analyzed by qRT-PCR in leaves (a) and shoot tips (b). (c,d) Expression of *CmGA20ox1* was analyzed by qRT-PCR in leaves (c) and shoot tips (d). (e) *In situ* hybridization of *CmGA20ox1* in chrysanthemum apical meristems at LT5 and at LT5 + N1. Plants grown under normal temperature for 5 and 6 weeks (C5 and C6) were used as controls. Scale bars, 200 μm. (f) *CmLFY* expression was analyzed by qRT-PCR in shoot tips. *UBIQUITIN* was used as the reference gene. The results are the means of three biological replicates with standard deviations. LT1–5, 1–5 weeks of low-temperature treatment. LT5 + N1, LT5 + N2, and LT5 + N5 indicate 1 week, 2 weeks, and 5 weeks of normal temperature after a 5-week low-temperature treatment, respectively.

CmMAF2 regulates flowering by regulating GA biosynthesis

To test whether *CmMAF2* plays a role in the regulation of flowering time, we used the 3′ region of the gene to specifically silence *CmMAF2* expression in chrysanthemum by RNA interference (RNAi) and generated a population of 36 *CmMAF2*-RNAi lines. Of these, we selected three for functional analysis based on their reduced *CmMAF2* expression levels, as determined by qRT-PCR analysis (Figure 4a). Since we did not find any other *MAF* homologs in our chrysanthemum transcriptome and public genome databases, we measured the expression of the other MADS-box gene family homologs *AGL8*, *AGL9*, *AGL104*, *SVP1*, and *SVP2*, whose functions have been associated with floral transition, in transgenic and wild-type (WT) plants, and confirmed that only the *CmMAF2* gene was silenced (Figure 4b).

We observed that under LD conditions, the plant heights of lines RNAi-24, RNAi-31, and RNAi-34 were 38 ± 1.0 cm, 34 ± 0.3 cm, and 33 ± 0.6 cm, respectively,

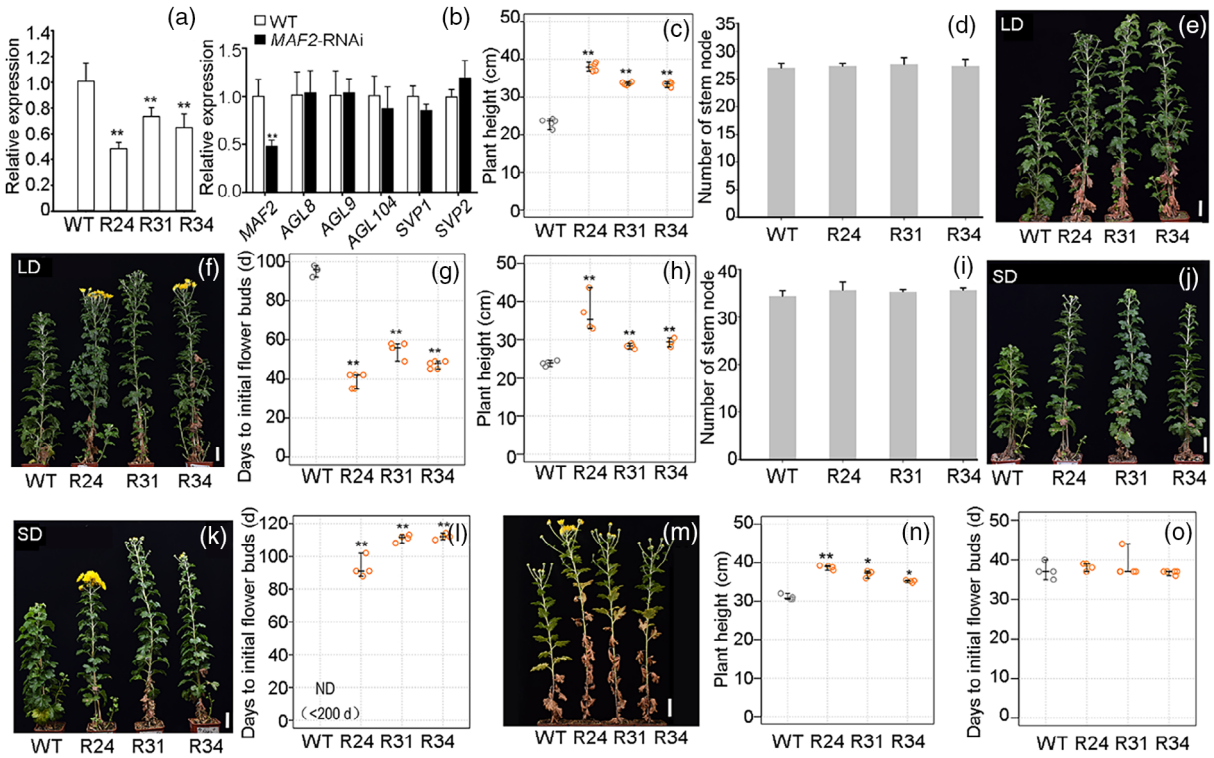

Figure 4. *CmMAF2*-RNAi plant flowering. (a,b) Expression of *CmMAF2* (a) and MADS-box family homologs (b) in WT and *CmMAF2*-RNAi plants as determined by qRT-PCR. *UBIQUITIN* was used as the internal control. (c,h) Plant heights of 4-week-old (c) and 12-week-old (h) WT and *CmMAF2*-RNAi plants grown under LD and SD conditions. (d,i) The number of stem nodes was recorded after 9 weeks of LD (d) and 18 weeks of SD (i) conditions. (e,j) Representative photographs of WT and *CmMAF2*-RNAi plants at flower bud emergence after 9 weeks of LD (e) and 18 weeks of SD (j) conditions. (f,k) Flower blooming in WT and *CmMAF2*-RNAi plants after 15 weeks of LD (f) and 20 weeks of SD (k) conditions. (g,l) Days until initial flower bud emergence in WT and *CmMAF2*-RNAi plants grown under LD (g) and SD (l) conditions. (m) Phenotypes of WT and *CmMAF2*-RNAi plants treated for 5 weeks with low temperature at week 16 after transplanting. (n) Plant heights of WT and *CmMAF2*-RNAi plants treated for 5 weeks with low temperature under LD conditions. (o) Days until initial flower bud emergence in WT and *CmMAF2*-RNAi plants treated for 5 weeks with low temperature under LD conditions. R24, R31, and R24 correspond to three independent *CmMAF2*-RNAi lines. The results are the means of three biological replicates with standard deviations. Asterisks indicate statistically significant differences (Student's *t*-test, $*P < 0.05$, $**P < 0.01$). Scale bars, 5 cm.

which were significantly greater than that of WT plants (23 ± 1.0 cm), but no obvious difference was observed in the numbers of stem nodes between the transgenic lines and WT plants (Figure 4c,d). Plants grown under SD conditions showed a similar trend (Figure 4h,i). We then monitored the flowering time of *CmMAF2*-RNAi and WT plants. Under LD conditions, the emergence of initial flower buds was observed at 39 ± 3.4, 55 ± 3.3, and 47 ± 1.8 days after transplanting in lines RNAi-24, RNAi-31, and RNAi-34, respectively, while flower buds emerged in WT plants at 96 ± 2.2 days. Meanwhile, the blooming time of transgenic lines was also earlier than in WT plants (Figure 4e–g). Under SD conditions, initial flower buds emerged at 93 ± 5.3, 111 ± 2.2, and 112 ± 1.6 days after transplanting in lines RNAi-24, RNAi-31, and RNAi-34, respectively, while no flower buds and blooming time were observed in WT plants until the end of the experiment (200 days after transplanting) (Figure 4j–l). We exposed the *CmMAF2*-RNAi lines and WT plants to a 5-week low-temperature treatment and observed a reduction in plant height, although *CmMAF2*-RNAi plants were still taller than the WT plants (Figure 4m,n). In addition, no significant difference in flowering time was observed between the *CmMAF2*-RNAi lines and WT plants (Figure 4m,o), suggesting that the low-temperature treatment mitigated the consequences of RNAi-mediated suppression of *CmMAF2* expression on flowering time.

To investigate whether *CmMAF2* affects flowering through the GA flowering pathway, we measured endogenous GA concentrations in *CmMAF2*-RNAi plants and observed that bioactive GA levels (GA_1 and GA_4) were significantly higher in *CmMAF2*-RNAi plants than in WT plants (Figure 5a). We then tested the effects of the GA biosynthesis inhibitor PAC on flowering time of *CmMAF2*-RNAi and WT plants. After PAC treatment, plant height was significantly reduced in the *CmMAF2*-RNAi and WT plants, but the degree of inhibition in *CmMAF2*-RNAi plants was lower than in WT plants (Figure 5b,c). Additionally, flowering time was delayed in both *CmMAF2*-RNAi and WT plants, and WT plants

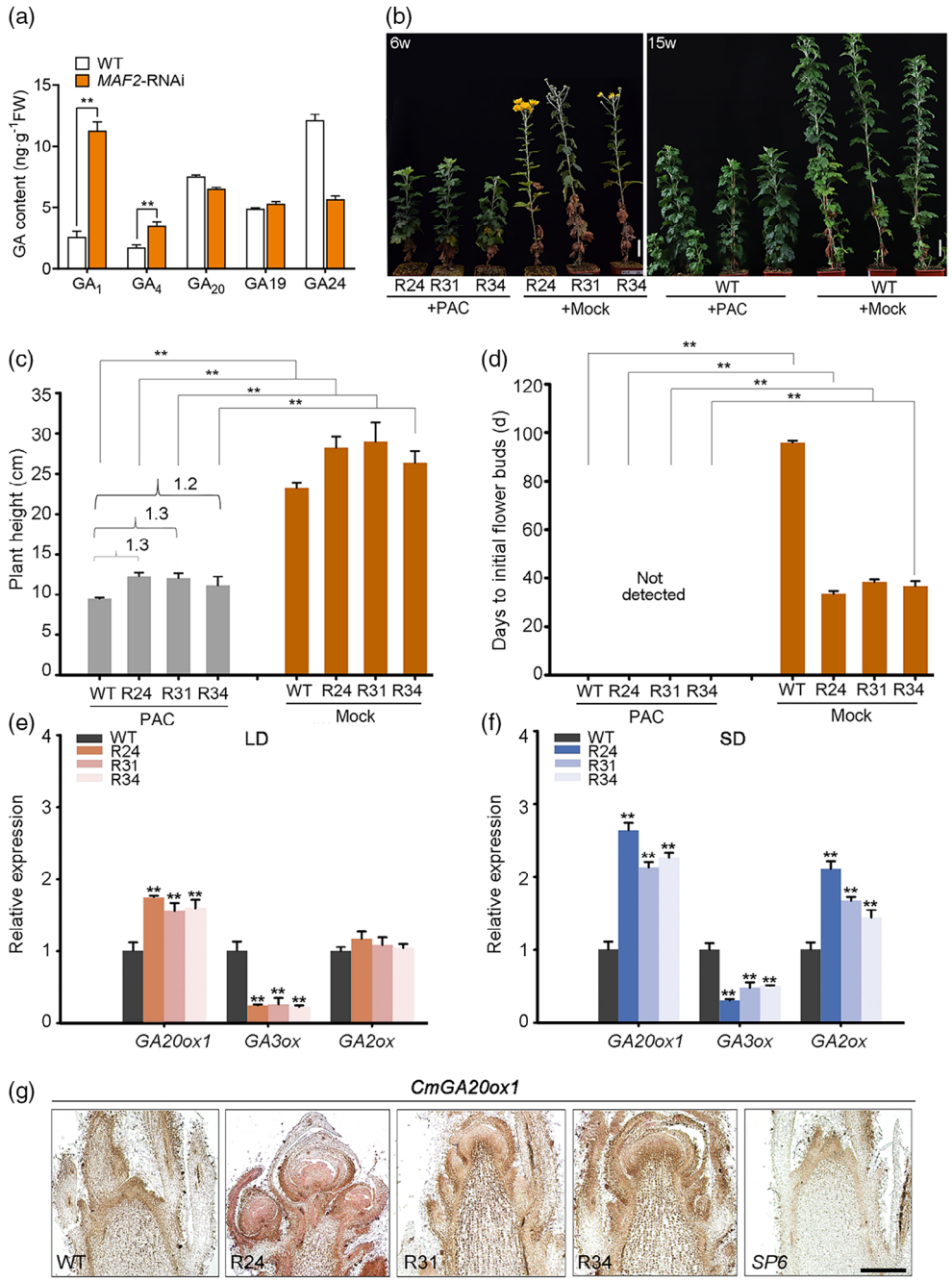

Figure 5. The effects of GAs on flowering in *CmMAF2*-RNAi and WT chrysanthemum plants. (a) GA contents in 10-week-old WT and *CmMAF2*-RNAi plants grown under LD conditions. (b) Phenotypes of *CmMAF2*-RNAi lines treated with the GA biosynthesis inhibitor PAC under LD conditions after 6 weeks and of WT plants treated with the GA biosynthesis inhibitor PAC under LD conditions after 15 weeks. Scale bars, 5 cm. (c) The effect of PAC treatment on the height of 5-week-old RNAi and WT plants. (d) Effects of PAC treatment on the time until initial flower bud emergence in RNAi and WT plants. R24, R31, and R24 correspond to three independent *CmMAF2*-RNAi lines. Mock treatment with 10% ethanol solution was used as a control. (e,f) Expression analyses of genes related to GA biosynthesis under LD (e) and SD (f) conditions, as determined by qRT-PCR. *UBIQUITIN* was used as an internal control. The results are the means of three biological replicates with standard deviations. (g) *In situ* hybridization analysis of *CmGA20ox1* expression in the apical meristems of WT and *CmMAF2*-RNAi plants grown under LD conditions. The negative control *SP6* was hybridized with the sense probe. Scale bars, 200 μm. The results are the means of three biological replicates with standard deviations. Asterisks indicate statistically significant differences (Student's *t*-test, $^{**}P < 0.01$).

showed a more substantial delay in flowering than *CmMAF2*-RNAi plants, such that we did not observe flower buds in WT plants for 100 days after treatment (Figure 5b–d). These results indicated that GA biosynthesis is involved in regulating *CmMAF2* expression and its effect on flowering.

CmMAF2 is a direct upstream regulator of the GA biosynthesis gene *CmGA20ox1*

To clarify whether CmMAF2 directly regulates genes involved in GA biosynthesis, we analyzed the expression of differentially expressed genes related to GA synthesis in the vegetative stage (1 w) and the early stage of floral transition (5 w) in both *CmMAF2*-RNAi transgenic and WT plants by qRT-PCR. We found that in the vegetative and early floral transition stages, the expression of *CmGA20ox1* was higher in *CmMAF2*-RNAi plants than in WT under both LD and SD conditions, but *CmGA3ox* expression was lower. We did not detect a significant difference in *CmGA2ox* expression between transgenic and WT plants under flowering-inductive LD conditions of the low temperature-induced chrysanthemum variety (Figure 5e,f; Figure S4a–c). *In situ* hybridization analysis of *CmGA20ox1* expression in apical meristems showed stronger labeling in RNAi plants than in WT plants, although the stages of inflorescence differentiation were different between the RNAi and WT plants (Figure 5g).

We noted that the *CmGA20ox1* promoter contains three annotated CArG-box motifs, while the *CmGA2ox* promoter does not contain any (Figure 6a; Figure S5). A yeast one-hybrid (Y1H) analysis to assess the interaction of CmMAF2 with each of the three motifs revealed that it bound to them all (Figure 6b). Next, we carried out an electrophoretic mobility shift assay (EMSA) to validate the interaction of CmMAF2 with the three CArG-box motifs and observed that a GST-tagged version of CmMAF2 (CmMAF2-GST) bound to each of the CArG-box-containing fragments that had been biotin-labeled. In this analysis, increasing the amounts of unlabeled cold probes significantly decreased the levels of CmMAF2 binding to biotin-labeled probes, whereas unlabeled mutant probes did not compete for CmMAF2 binding (Figure 6d). Finally, we assayed the activity of a dual-luciferase reporter to evaluate the regulatory effects of CmMAF2 on the *CmGA20ox1* promoter *in vivo*. Tobacco (*Nicotiana benthamiana*) leaf cells co-expressing *CmMAF2* and the *CmGA20ox1* promoter had a significantly lower LUC/REN ratio than leaf cells transformed with *CmMAF2* alone, the *CmGA20ox1* promoter alone, or a mutated *GA20ox1* promoter (Figure 6c), suggesting that CmMAF2 directly represses the expression of *CmGA20ox1*.

To confirm that CmMAF2 influences flowering by directly regulating the expression of *CmGA20ox1*, we silenced *CmGA20ox1* in WT and *CmMAF2*-RNAi plants using a modified cabbage leaf-curl geminivirus vector (CaLCuV) containing the artificial microRNA-CmGA20ox1 (CaLCuV-amiR-CmGA20ox1) (Figure 6e). We observed that under LD conditions, compared with WT-CaLCuV plants, silencing *CmMAF2* alone significantly increased the plant height, and silencing *CmGA20ox1* alone strongly reduced plant height, while double silencing of *CmMAF2* and *CmGA20ox1* recovered the plant height close to that of WT-CaLCuV plants (Figure 6f,g). We also observed the influence of flowering under LD conditions compared with early flowering of *CmMAF2*-RNAi-CaLCuV plants; both the time until initial flower bud emergence and the time until blooming were significantly longer in *CmMAF2* and *CmGA20ox1* double silenced plants, which were close to those of WT-CaLCuV plants. Silencing *CmGA20ox1* alone delayed flowering extremely much, and we did not even observe flower opening (Figure 6h,i).

Collectively, these data indicate that *CmMAF2* affects GA levels to regulate floral transition by directly targeting *CmGA20ox1*.

CmC3H1 directly activates *CmMAF2* expression in response to low temperatures

To investigate the upstream regulatory mechanism of *CmMAF2*, we first used different promoter regions of *CmMAF2* to screen the Y1H library. We found that a CCCH-type zinc-finger protein-encoding gene, *CmC3H1*, was a potential upstream candidate gene. Then, we measured the expression levels of *CmC3H1* in leaves and shoot tips. The results showed that as a general trend, the expression pattern of *CmC3H1* was consistent with that of *CmMAF2* (Figure 3a,b). Namely, the expression of *CmC3H1* was upregulated during low-temperature treatments and then downregulated after returning to normal temperatures in both leaves and shoot tips (Figure 7a,b).

Next, we performed a Y1H assay to confirm the interaction between CmC3H1 and the *CmMAF2* promoter. The results showed CmC3H1 bound to the third fragment of the *CmMAF2* promoter (Figure 7c). A chromatin immunoprecipitation assay coupled with PCR (ChIP-PCR) showed that CmC3H1 independently bound to the P5 or P6 fragment of the *CmMAF2* promoter (Figure 7d). We also assayed the activity of a dual-luciferase reporter to evaluate the regulatory activity of CmC3H1 on the *CmMAF2* promoter *in vivo*. *Nicotiana benthamiana* leaf cells co-expressing CmC3H1 and the *CmMAF2* promoter had a significantly higher LUC/REN ratio than leaf cells transformed with CmC3H1 or the *CmMAF2* promoter alone, suggesting that CmC3H1 directly activated the expression of *CmMAF2* (Figure 7e,f).

Finally, to verify the involvement of CmC3H1 in regulation of flowering, we transiently silenced *CmC3H1* in chrysanthemum plants (Figure 7g). We observed that under LD conditions, compared with control plants, both the time to initial flower bud emergence and the time to blooming were significantly reduced in *CmC3H1* silencing plants (Figure 7h,i). In addition, we evaluated the expression of *CmMAF2* and *CmGA20ox1*. Compared with the control plants, *CmMAF2* expression was significantly

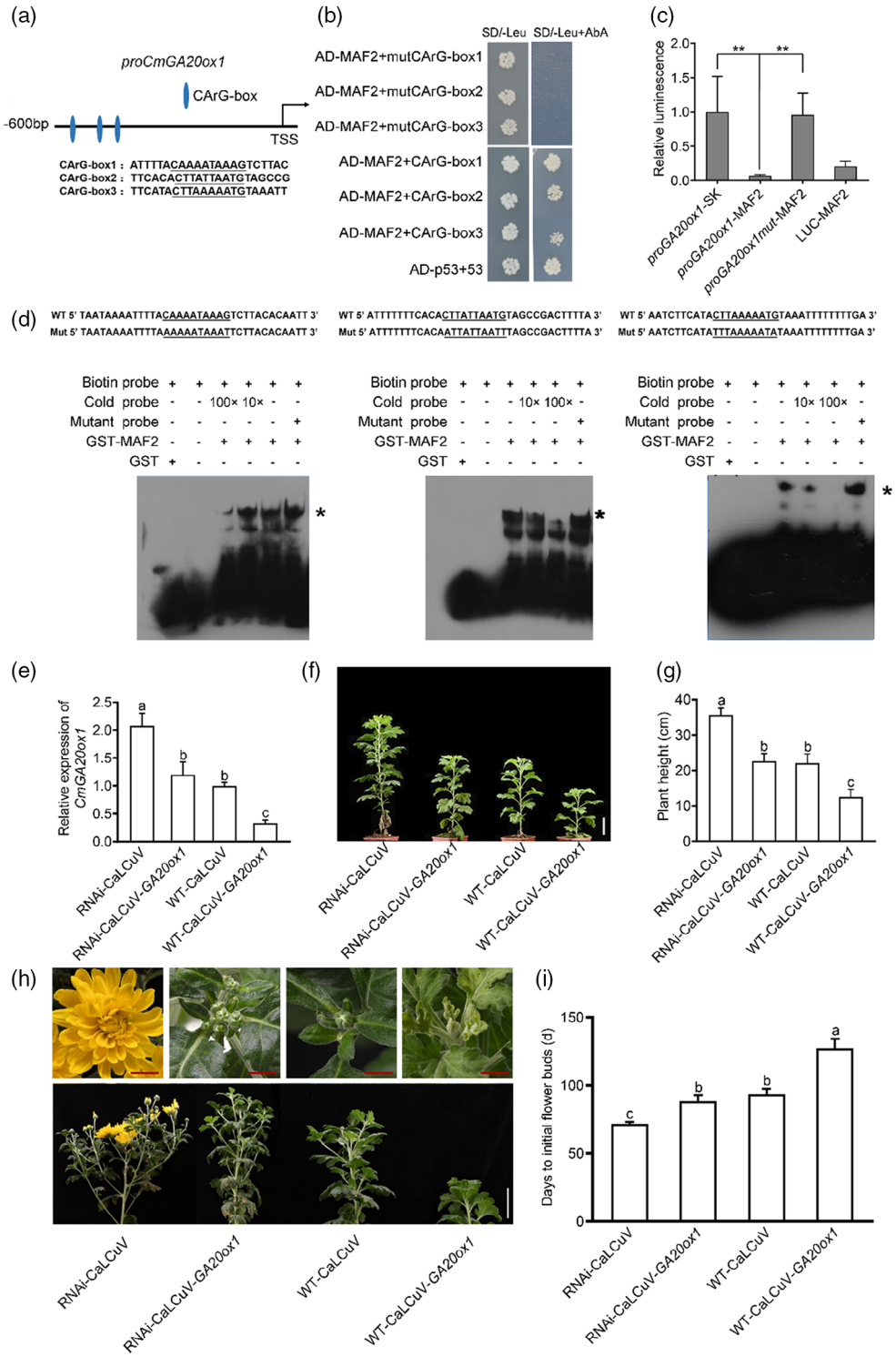

downregulated, while *CmGA20ox1* expression was significantly upregulated in *CmC3H1* silenced plants (Figure 7j).

Together, these results demonstrate that CmC3H1 could regulate the expression of *CmMAF2* positively and *CmGA20ox1* negatively, suggesting that the C3H1–MAF2 module might regulate flowering in response to low temperature by repressing GA biosynthesis in temperature-sensitive chrysanthemum ecotypes.

Figure 6. CmMAF2 represses the expression of *CmGA20ox1* by binding to its promoter. (a) Schematic representation of three CArG-box sequences and their positions in the 600-bp sequence immediately upstream from the *CmGA20ox1* transcription start site (TSS). (b) Interaction between CmMAF2 and the three CArG-boxes in the *CmGA20ox1* promoter, shown by a Y1H assay. The p53-AbAi bait vector and the p53 fragment prey vector were used as positive controls. All interactions were examined on SD/−Leu medium supplemented with 100 mg μl^{-1} AbA. (c) CmMAF2 affects the transcriptional activity of *CmGA20ox1*, as shown using a dual-luciferase reporter assay in *Nicotiana benthamiana* leaves. A 680-bp *CmGA20ox1* promoter sequence was used. *mPro-GA20ox* is the same promoter fragment with the three CArG *cis*-elements mutated. LUC indicates the pGreenII 0800-LUC empty vector containing the *REN* gene under the control of the 35S promoter. SK indicates the empty pGreenII 0029 62-SK vector. Samples were infiltrated into *N. benthamiana* leaves, and LUC and REN activities were assayed 3 days after infiltration. Three independent experiments were performed, and error bars indicate standard deviation. (d) The interaction of CmMAF2 and biotin-labeled CArG *cis*-elements as shown by EMSA. The oligonucleotide sequences of three CArG-boxes from the *CmGA20ox1* promoter were used as probes. The core sequences are underlined. The purified protein (2 μg) was incubated with 40 nmol of labeled WT or mutated probes. Non-labeled probes at various concentrations (10–100-fold) were added for the competition test. (e) Transcript abundance of *CmGA20ox1* in WT and *CmMAF2*-RNAi plants infected with CaLCuV or CaLCuV-amiR-CmGA20ox1. (f,h) Representative photographs of WT and *CmMAF2*-RNAi plants infected with CaLCuV or CaLCuV-amiR-CmGA20ox1 after 15 weeks of growth (f) and at flower blooming (h) under LD conditions. (g,i) Plant heights (g) and days to initial flower bud emergence (i) were recorded ($n > 5$). Error bars indicate standard deviation. Asterisks indicate significant differences according to a Student's *t*-test (*$P < 0.05$, **$P < 0.01$). Different letters indicate significant differences according to Duncan's multiple range test ($P < 0.05$). Red scale bars, 1 cm; white scale bars, 5 cm.

DISCUSSION

Over time, chrysanthemum has evolved into multiple ecotypes, some of which are more sensitive to the photoperiod, while others are more sensitive to temperature. On the one hand, the photoperiod influences flowering time based on the critical day length for flowering (Kawata, 1987), mainly through affecting the expression of *BBX24* and *AFT*/*FTL3* in the gene regulatory network (Higuchi et al., 2013; Yang et al., 2014). On the other hand, low temperatures affect floral induction via two different pathways. One of the pathways is that low temperatures inhibit floral induction, and low temperature-treated plants appeared to be less sensitive to SD conditions (Hisamatsu et al., 2017; Vegis, 1964). The other pathway is that prolonged low-temperature exposure can break the dormant state of the meristem and induce flowering. The low-temperature requirement for flowering competence is also called 'vernalization' (Schwabe, 1950). However, little is known about the underlying molecular mechanisms by which temperature-sensitive chrysanthemum initiates flowering in response to low temperatures. Our current work provides a novel molecular framework: the C3H1–MAF2 module responds to low temperatures to induce flowering in temperature-sensitive chrysanthemum. Under low-temperature conditions, *CmMAF2* expression was upregulated by CmC3H1 to repress the expression of *CmGA20ox1* and reduced the levels of bioactive GAs. When returning to warm temperatures, *CmMAF2* expression was reduced, the expression of *CmGA20ox1* was induced, and high bioactive GA levels rapidly induced *CmLFY* expression, thereby initiating floral transition (Figure 8).

Cys_3His-type zinc finger proteins have been reported to play critical roles in a broad range of processes, such as plant growth, development, and stress responses, in Arabidopsis (Bogamuwa & Jang, 2014). However, the mechanisms underlying the roles of C3H1 in regulating flowering time in response to low temperatures remained unknown. In the present work, *CmC3H1* expression was significantly upregulated upon exposure to low temperatures in a temperature-sensitive chrysanthemum ecotype. CmC3H1 activated the expression of the downstream gene *CmMAF2* by directly binding to its promoter region. Both *CmC3H1* and *CmMAF2* expression decreased rapidly after returning to warm temperatures. Hence, we conclude that CmC3H1 acts directly upstream of *CmMAF2* and plays important roles in regulating flowering time in response to low temperatures.

Floral transition in the low temperature-sensitive chrysanthemum ecotype requires low-temperature exposure, which is also referred to as 'vernalization' (Schwabe, 1950). In *A. thaliana*, *AtFLC* expression was reported to be gradually downregulated during vernalization, and the flowering process was completed at these low expression levels after low-temperature treatments (Whittaker & Dean, 2017). *AtMAF2* is considered to be one of the close homologs to *AtFLC*, which regulates flowering time in response to vernalization (Gu et al., 2013; Ratcliffe et al., 2003). However, our present results show that the expression pattern of *CmMAF2* in response to low temperatures is completely different from that of *AtFLC*. In temperature-sensitive chrysanthemum, *CmMAF2* expression was upregulated during low-temperature treatment and downregulated when normal temperatures were sensed (Figure 3a,b). Besides, CmMAF2 can directly target the GA biosynthesis gene *CmGA20ox1* and regulate the biosynthesis of bioactive GAs. After long-term exposure to low temperatures, the plants showed early flowering due to increased levels of bioactive GAs (Figure 1d,e; Figure 2a). Prolonged exposure to low temperature appears to induce flowering in this ecotype. Application of exogenous GAs can promote flowering in chrysanthemum (Figure 2b–d) (Yang et al., 2014). On the contrary, reducing GA levels with PAC delays flowering (Figure 5b–d). Hence, GA is a prominent phytohormone promoting floral induction in the temperature-sensitive chrysanthemum ecotype. Meanwhile, GA can circumvent the prolonged low-temperature requirements for flowering.

The relationship between low temperatures and GA levels has been elucidated in several plant species. For

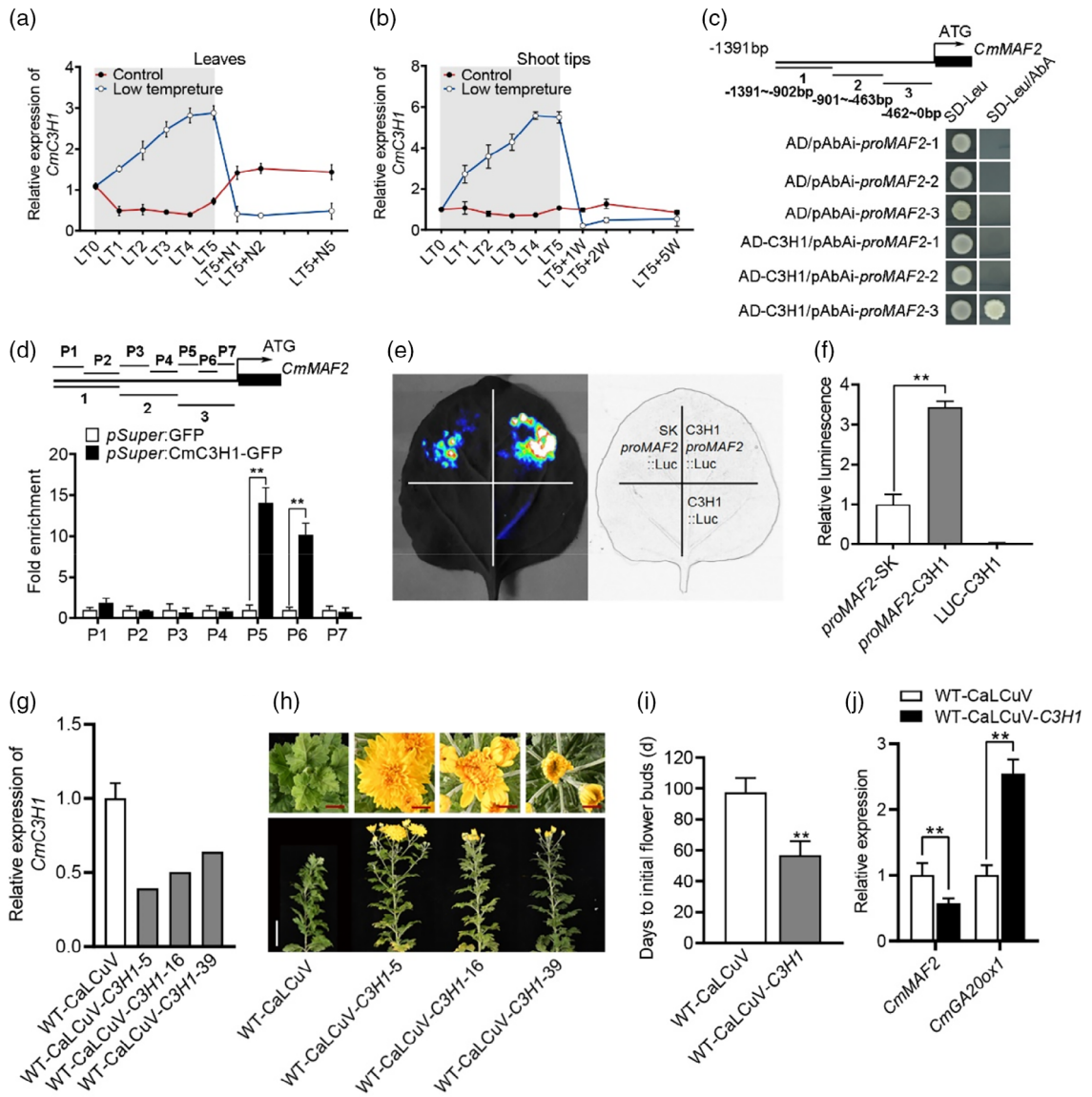

Figure 7. CmC3H1 directly activates *CmMAF2* expression in response to low temperatures. (a,b) Expression of *CmC3H1* was analyzed by qRT-PCR in leaves (a) and shoot tips (b). (c) Interaction between CmC3H1 and different regions in the *CmMAF2* promoter, as shown by a yeast one-hybrid assay. All interactions were examined on SD/−Leu medium supplemented with 100 mg μl^{-1} AbA. (d) ChIP analysis of the indicated fragments (P1–P7) in the *CmMAF2* promoter. The chromatin of *pSuper*::*CmC3H1*-GFP chrysanthemum plants was immunoprecipitated with an anti-GFP antibody and *pSuper*::GFP chrysanthemum plants served as a negative control. The amount of the indicated DNA fragment was determined by qRT-PCR and normalized to the *pSuper*::GFP control (set to 1 for each fragment). (e,f) Interaction between CmC3H1 and the *CmMAF2* promoter, as shown using a dual-luciferase reporter assay in *Nicotiana benthamiana* leaves. A 774-bp *CmMAF2* promoter sequence was used. Representative photographs of firefly luciferase fluorescence signals are shown in (e) and the relative LUC/REN ratio is shown in (f). (g) Transcript abundance of *CmC3H1* in transiently *CmC3H1*-silenced chrysanthemum plants. (h) Representative photographs of WT plants infected with CaLCuV or CaLCuV-amiR-CmC3H1 after 14 weeks of flower blooming under LD conditions. (i) Days to initial flower bud emergence were recorded ($n > 5$). (j) Expression of *CmMAF2* and *CmGA20ox1* in transiently *CmC3H1*-silenced chrysanthemum plants. Error bars indicate standard deviation. Asterisks indicate significant differences according to a Student's *t*-test (**$P < 0.01$). Red scale bars, 1 cm; white scale bars, 5 cm.

example, in radish (*Raphanus sativus*) and field pennycress (*Thlaspi arvense*), the application of exogenous GA_3 can substitute for the vernalization requirement (Metzger, 1985; Suge & Rappaport, 1968), and in winter canola, GA levels increase at the end of vernalization (Zanewich & Rood, 1995). In the herbaceous perennial *A. alpine*, PEP1, another MAF2 homolog, regulates GA metabolism by binding to *GA2ox* rather than *GA20ox*. Additionally, in *A. alpine*, GA does not overcome the vernalization requirement but reduces the duration of the vernalization time needed. Bioactive GA_1 levels are unchanged during or after vernalization, whereas GA_4 levels are reduced during vernalization and then increase after vernalization (Tilmes et al., 2019). Our experiments showed that in the

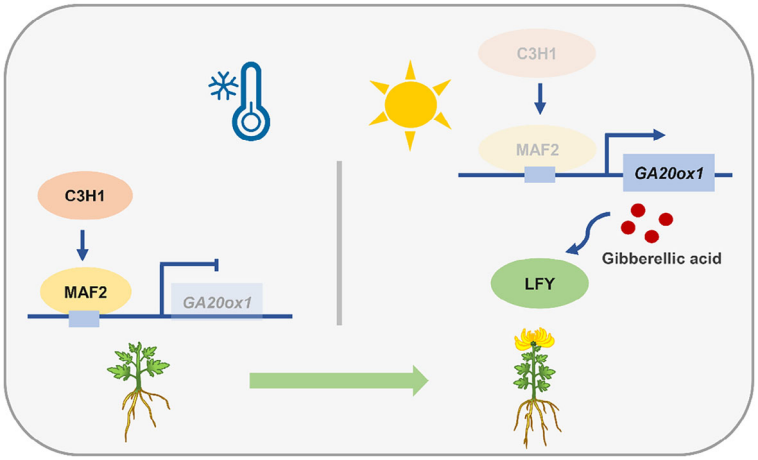

Figure 8. A schematic model describing the C3H1–MAF2 module and its response to low temperatures to induce flowering in temperature-sensitive chrysanthemum ecotypes. Under low-temperature conditions, *CmMAF2* expression is upregulated by CmC3H1 to repress the expression of *CmGA20ox1*, reducing bioactive GA levels. When returning to warm temperatures, *CmMAF2* expression is reduced to release the expression of CmGA20ox1, and high bioactive GA levels rapidly induce *CmLFY* expression, thereby initiating floral transition.

temperature-sensitive chrysanthemum ecotype, CmMAF2 regulates GA metabolism under low-temperature conditions by binding to *CmGA20ox1*, causing a reduction in the levels of both bioactive GA_1 and GA_4. Meanwhile, in *CmMAF2*-silenced transgenic plants, bioactive GA_1 and GA_4 levels increased, contributing to early flowering (Figure 5a). When GA levels were reduced by PAC treatment, the transgenic plants showed reversed phenotypes. Hence, in the temperature-sensitive chrysanthemum ecotype, both GA_1 and GA_4 levels affect floral induction. Collectively, the GA metabolism in response to low temperatures is distinct between chrysanthemum and other species.

It has been reported that three FT-like genes (*CsFTL1*, *CsFTL2*, and *CsFTL3*) play important roles in photoperiod-sensitive chrysanthemum, and their expression is induced by SD signals regulating floral transition via the photoperiod pathway (Higuchi et al., 2013). However, our present results showed that in temperature-sensitive chrysanthemum, *CmLFY* is the critical floral gene responsible for integrating the low-temperature and GA pathways.

MATERIALS AND METHODS

Plant materials and growth conditions

Chrysanthemum (*C. morifolium* cv. Summer Yellow), which has a low-temperature sensitivity, was used in this study. Plants were propagated on half-strength Murashige and Skoog (1/2 MS) medium for 30 days before being transplanted into 9 cm diameter pots containing a 3:1 (v/v) mixture of peat and vermiculite. For LD conditions, plants were grown in a culturing room at 23 ± 1°C, with a relative humidity of 40% and 100 μmol m^{-2} sec^{-1} illumination with fluorescent lamps (16 h light/8 h dark). For SD treatments, plants were transferred to a culturing room with an 8 h light/16 h dark regime and the same humidity and light quality.

Treatments

For low-temperature treatments, plants were transferred to a 4 ± 1°C chamber under either LD conditions for 5 weeks or SD conditions for 8 weeks and then transferred back to normal temperature under SD or LD conditions. To observe the phenotype in the field, the plants were treated with 5 weeks of low temperature (4 ± 1°C) in a chamber and then transferred to the Shangzhuang Experimental Station of China Agricultural University in May (Beijing, China). For GA treatments, plants were sprayed after transplanting with 10 μM or 100 μM $GA_{4/7}$ (Sigma Aldrich, Saint Louis, MO, USA) and grown under either LD or SD conditions at 23 ± 1°C. $GA_{4/7}$ was dissolved in 10% ethanol, and the same ethanol concentration was used as a mock control. Plants were sprayed with $GA_{4/7}$ twice a week for 2 months. For PAC treatment, both *CmMAF2*-RNAi transgenic and WT plants were sprayed with 250 mg L^{-1} PAC (Sigma Aldrich) twice a week for 5 weeks. PAC was dissolved in 1% dimethyl sulfoxide (DMSO), and the same concentration of DMSO without PAC was used as a mock control.

Gene cloning

We obtained full-length *CmMAF2*, *CmC3H1*, and *CmGA20ox1* cDNA using the SMART™ RACE cDNA amplification kit (Clontech, Shiga-ken, Japan) according to the manufacturer's instructions. Genomic DNA was extracted from chrysanthemum leaves using the cetyltrimethyl ammonium bromide method (Huang et al., 2000), and promoters were cloned using inverse PCR and thermal asymmetric interlaced PCR with 2X M5 HiPer plus Taq HiFi PCR mix (Mei5 Biotech, China) (Liu & Chen, 2007). All primers used are listed in Table S1.

Sequence analysis

The conserved MADS-box and zinc-finger domains were predicted using InterProScan (Jones et al., 2014). Multiple amino acid sequences were aligned using ClustalW (Thompson et al., 1994) with default parameters, and the result is shown in BioEdit format (Hall, 1999). The phylogenetic tree was constructed using the neighbor-joining algorithm with 1000 bootstrap replicates using MEGA 5.0 software (Tamura et al., 2011). The protein sequences of CmMAF2 homologs were identified in the National Center for Biotechnology Information (NCBI) database. The *cis*-elements in the *CmGA20ox1* and *CmGA2ox1* promoters were analyzed using the PlantCARE program (Lescot et al., 2002).

qRT-PCR analysis

Tips of the fourth expanded leaves were collected from five replicates for each sample at Zeitgeber time 10 (ZT10). Total RNA was

extracted using the RNAiso Plus reagent (TaKaRa, Japan) according to the manufacturer's instructions. One microgram of total RNA was reverse transcribed to cDNA using the HiScript II Q Select RT SuperMix for qPCR (+gDNA wiper) kit (Vazyme Biotech Co., Ltd, China), and qRT-PCR (in a volume of 20 μl containing 2 μl cDNA as the template) was carried out using the StepOne Real-Time PCR System (Applied Biosystems, USA) in standard mode with a KAPA SYBR FAST Universal qRT-PCR Kit (Kapa Biosystems, USA). The chrysanthemum *UBIQUITIN* gene (GenBank accession NM_112764) was used as an internal control. Relative expression was calculated using the $2^{-\Delta\Delta Ct}$ method (Livak & Schmittgen, 2001). The gene-specific primers are listed in Table S1.

Chrysanthemum transformation

To generate the RNAi vector, 305-bp *CmMAF2*-specific sense and antisense fragments were amplified using two pairs of primers containing either *Asc*I/*Swa*I or *Pac*I/*Bam*HI sites. The resulting PCR products were digested with the abovementioned restriction enzymes and then inserted into the binary vector PFGC1008 digested with the same enzymes to form an intron-containing 'hairpin' RNA construct containing the cauliflower mosaic virus 35S promoter. This plasmid was then introduced into *Agrobacterium tumefaciens* strain EHA105 by the freeze–thaw method and transformed into chrysanthemum by *A. tumefaciens*-mediated transformation. Each explant for transformation (1.0 cm × 1.0 cm square leaf) was derived from a young chrysanthemum leaf and pre-cultured on MS medium for 3 days. After agro-infiltration, the explants were placed under dark conditions for 2 days. Next, the infected explants were washed gently in washing medium (4.4 g L^{-1} MS medium, 30 g L^{-1} sucrose, 200 mg L^{-1} cefotaxime, pH 5.8) and transferred to shoot-inducing medium (4.4 g L^{-1} MS medium, 30 g L^{-1} sucrose, 0.3 g L^{-1} 1-naphthaleneacetic acid [NAA], 3.0 g L^{-1} 6-benzylaminopurine [6-BA], 200 mg L^{-1} cefotaxime, 1.0 mg L^{-1} hygromycin B, 6.4 g L^{-1} agar, pH 5.8) for 3 days. The medium was changed every 2 weeks. Elongated shoots were placed into rooting medium (4.4 g L^{-1} 1/2 MS medium, 30 g L^{-1} sucrose, 0.02 mg L^{-1} NAA, 200 mg L^{-1} cefotaxime, 1.0 mg L^{-1} hygromycin B, 7.8 g L^{-1} agar, pH 5.8) after 30 days.

Phenotypic measurements

To evaluate the time until initial flower bud emergence, the day of transplanting was set as day 1. The time of the first visible flower buds (2 mm diameter) was then recorded. The shoot apex and inflorescence were dissected from the chrysanthemum under a light microscope (Leica DFC450, Germany). After dissection, samples were immediately observed by scanning electron microscopy (Hitachi S-4700, Japan) with an acceleration voltage of 2 kV.

Determination of GA contents

The shoot apex of *CmMAF2*-RNAi or WT plants was collected in three replicates at ZT10. GA contents were determined by a commercial company (Metware Biotechnology Co., Ltd., Wuhan, China) using the AB Sciex QTRAP 6500 liquid chromatography–tandem mass spectrometry platform. Raw data were analyzed by Analyst 1.6.3 software (AB Sciex, Waltham, MA, USA).

RNA-seq analysis

Total RNA samples were extracted from the top four expanded leaves of WT plants grown at low temperature for 5 weeks and after 1 week or 5 weeks of returning to normal conditions. Three biological replicates were collected for each time point. RNA-seq libraries were prepared (Zhong et al., 2011) and sequenced using the HiSeq 2000 (Illumina) platform at Novogene Co. Ltd. (Beijing, China, http://www.novogene.com/). RNA-seq data were processed, assembled, and annotated as previously described (Wei et al., 2017).

EMSA

EMSA was performed using the LightShift Chemiluminescent EMSA Kit (Thermo Fisher) according to the manufacturer's instructions with minor modifications. Briefly, the PGEX-4 T-2-CmMAF2 recombinant vector was used to express the GST-CmMAF2 fusion protein before purification as previously described (Liu et al., 2017). Next, 40 nmol of labeled WT or mutated probes was incubated with 2 μg of protein in 20 μl reaction buffer (2 μl of 10× binding buffer, 1 μl of 1 μg μl^{-1} poly(dI:dC), 1 μl of 50% glycerol, 1 μl of 1% NP-40, and 10 mM ethylenediaminetetraacetic acid) at 25°C for 30 min. Complementary biotin-labeled, mutated, and unlabeled 3′ end DNA oligonucleotides were synthesized and annealed. Unlabeled DNA was used as a competitor probe. The probe sequences are shown in Table S1.

Yeast one-hybrid assay

Protein and DNA interactions in yeast cells were determined using the Matchmaker™ Gold Yeast One-Hybrid Library Screening System (Clontech, Japan). To test whether CmMAF2 binds to the promoter of *CmGA20ox1*, the *CmMAF2* full-length sequence was inserted into the pGADT7 vector, and the *CmGA20ox1* promoter and mutated fragments were inserted into the pAbAi vector (Clontech, Japan). Interactions were examined on SD/−Leu medium with 100 mg μl^{-1} aureobasidin A (AbA) (Clontech, Japan). To identify the upstream gene of *CmMAF2*, we created a Y1H library using high-quality chrysanthemum cDNA. Then, the promoter sequence of *CmMAF2* was divided into three fragments and inserted into the pAbAi vector. After screening the Y1H library, we confirmed the screening results. Primers used are shown in Table S1.

Dual-luciferase reporter assay in *N. benthamiana*

To investigate whether CmMAF2 regulates *CmGA20ox1* directly *in vivo*, we used the pGreenII 0800-LUC and pGreenII 0029 62-SK vectors (Hellens et al., 2005). A 680-bp *CmGA20ox1* promoter sequence and the same sequence with three mutated cArG-boxes were inserted into the *Bam*HI/*Nco*I sites of the pGreenII 0800-LUC vector. The *CmMAF2* coding sequence was amplified by PCR and inserted into the pGreenII 62-SK vector using *Bam*HI and *Kpn*I. Similarly, to investigate whether CmC3H1 regulates *CmMAF2* directly *in vivo*, a 774-bp *CmMAF2* promoter sequence was inserted into the *Hin*dIII/*Bam*HI sites of the pGreenII 0800-LUC vector, and the *CmC3H1* coding sequence was inserted into the pGreenII 62-SK vector using *Eco*RI and *Kpn*I.

All constructs were transformed into *A. tumefaciens* strain GV3101 harboring the pMP90 and pSoup plasmids (Hellens et al., 2000). *Nicotiana benthamiana* plants with three to five young leaves grown at 22°C under LD conditions were used as materials. Mixtures of *A. tumefaciens* cultures expressing either the coding sequence or the promoter fragments (v:v, 1:5) were infiltrated into *N. benthamiana* leaves using a needleless syringe (Wei et al., 2017). LUC and REN activities were measured using dual-luciferase reporter assay reagents (Promega, USA) and a Glo-Max 20/20 luminometer (Promega, USA). The ratios of LUC and REN are expressed as activation or repression. The LUC images were taken using an iKon-L936 imaging system (Andor Tech, Belfast, UK).

Chromatin immunoprecipitation (ChIP) assay

Chromatin immunoprecipitation experiments were carried out following a previously described protocol (Saleh et al., 2008). The full-length sequence of *CmC3H1* without the stop codon was inserted into the pSuper1300 (GFP-C) vector using *Xba*I and *Kpn*I. The resulting constructs and empty vector control were separately introduced into *A. tumefaciens* strain EHA105. Afterward, *Agrobacterium* cultures were harvested by centrifugation, resuspended in infiltration buffer (10 mM MES, 10 mM $MgCl_2$, and 200 mM AS, pH 5.6) to a final OD_{600} of 1.0, and infiltrated into chrysanthemum leaves using a needleless syringe. After 3 days, approximately 1.5 g of young leaves was fixed by incubation in 1% formaldehyde under vacuum for 10 min. The reaction was stopped by adding 2.5 ml 2 M glycine (0.125 mM final concentration) for another 5 min under vacuum. The leaves were washed twice with deionized water and frozen in liquid nitrogen. Chromatin was then extracted and sonicated, followed by overnight immunoprecipitation using anti-GFP (BE2001, Easybio, Beijing, China) and Magna ChIP™ Protein A + G Magnetic Beads (EMD Millipore, USA). The co-precipitated DNA was purified with a QIAquick PCR Purification Kit (Qiagen GmbH, Germany). qRT-PCR was conducted to measure the enrichment of DNA fragments. Primers are listed in Table S1.

In situ hybridization

Shoot apices were fixed in 3.7% formalin–acetic acid–alcohol overnight. Specific *CmGA20ox1* probes were designed according to the 3′ untranslated region. Sense and antisense probes were synthesized using SP6 and T7 RNA polymerase, respectively. *In situ* hybridization experiments were performed as previously described (Zhang et al., 2013). Primers are listed in Table S1.

Virus-induced gene silencing

To silence *CmGA20ox1* and *CmC3H1* in chrysanthemum, a previously reported virus-based microRNA expression system was used (Tang et al., 2010; Xu et al., 2020). A modified CaLCuV vector containing pre-cmo-GA20ox1 (CaLCuV + GA20ox1) and pre-cmo-C3H1 were generated and introduced into *A. tumefaciens* strain GV3101. The transformed *A. tumefaciens* cultures were inoculated overnight in LB medium and resuspended in infiltration buffer to a final OD_{600} of 1.5.

Then, the cultures containing pCVB and CaLCuV- GA20ox1 or pCVB and CaLCuV (control) were mixed in a 1:1 ratio (v/v) and incubated in the dark at 28°C for 3–4 h before vacuum infiltration. Fifty-day-old WT and RNAi-CmMAF2 plants immersed in infiltration buffer were vacuum-treated (−0.7 MPa) for 3 min. Similar to the previous treatment, 50-day-old WT plants immersed in infiltration buffer containing pCVB and CaLCuV- C3H1 or pCVB and CaLCuV (control) were vacuumed (−0.7 MPa) for 3 min. Then, the plants were placed in the dark at 8°C for 3 days and transplanted into pots filled with a 1:1 (v/v) mixture of peat:vermiculite and grown at 23 ± 1°C under LD conditions. The silenced plants were validated by RT-qPCR to determine the expression of *CmGA20ox1* or *CmC3H1*. Three independent experiments were performed, and at least six positive plantlets were used to observe the phenotypes.

ACCESSION NUMBERS

Sequences can be found under the following accession numbers: *CmMAF2* (MN255845), *CmC3H1* (OM963136), the promoter sequence of *CmGA20ox1* (MN255846), *AtFLC* (AT5G10140), *AtMAF1* (AT1G77080), *AtMAF2* (AT5g65050), *AtMAF3* (AT5G65060), *AtMAF4* (AT5G65050), *AtMAF5* (AT5G65080), *RsFLC* (AJN00653), *AtSVP* (AT2G22540), *AtFUL* (*AT5G60910*), *BvFL1* (DQ189210), *BnFLC* (AFU61576).

AUTHOR CONTRIBUTIONS

JL, XZ, and BH conceived and designed the experiments; JL performed most of the experiments; YZ and ZW contributed to the chrysanthemum transformation; AP, YX, HH, and RZ contributed to GA treatment experiments; AP observed apex development using scanning electron microscopy; AP and ZG conducted real-time PCR experiments; CM, CJ, SG, JG, and BH provided technical support and conceptual advice; JL and XZ analyzed the data; BH and JL wrote the manuscript.

ACKNOWLEDGMENTS

We thank PlantScribe (www.plantscribe.com) and Dr. Puneet Paul (University of Nebraska Lincoln) for carefully editing this manuscript. This work was supported by the National Key Research and Development Program of China (Grant No. 2018YFD1000400), the National Natural Science Foundation of China (Grant Nos. 32030096, 31772347, and 31822045), and the Construction of Beijing Science and Technology Innovation and Service Capacity in Top Subjects (CEFF-PXM2019_014207_000032).

CONFLICT OF INTEREST

The authors declare that there is no conflict of interest.

DATA AVAILABILITY STATEMENT

All data included in this study are available upon request by contact with the corresponding author.

SUPPORTING INFORMATION

Additional Supporting Information may be found in the online version of this article.

Data S1. Differentially expressed genes in chrysanthemum after 5 weeks of low-temperature treatment (LT5).

Figure S1. Effects of low temperature on flowering under short-day (SD) conditions and scanning electron micrographs showing apex development under low-temperature, long-day (LD) conditions.

Figure S2. Effects of exogenous gibberellin ($GA_{4/7}$) treatment on flowering under SD conditions.

Figure S3. CmMAF2 sequence alignment and *CmGA20ox2* expression.

Figure S4. *CmGAox* expression at different developmental stages.

Figure S5. *cis*-Element analyses of the *CmGA2ox* promoter (approximately 900 bp upstream from the start codon).

Table S1. Primers used in this study.

REFERENCES

Amasino, R. (2004) Vernalization, competence, and the epigenetic memory of winter. *The Plant Cell*, **16**, 2553–2559.

Amasino, R. (2009) Floral induction and monocarpic versus polycarpic life histories. *Genome Biology*, **10**, 228.

Barreda, V.D., Palazzesi, L., Telleria, M.C., Olivero, E.B., Raine, J.I. & Forest, F. (2015) Early evolution of the angiosperm clade Asteraceae in the

cretaceous of Antarctica. *Proceedings of the National Academy of Sciences of the United States of America*, **112**, 10989–10994.

Binenbaum, J., Weinstain, R. & Shani, E. (2018) Gibberellin localization and transport in plants. *Trends in Plant Science*, **23**, 410–421.

Bogamuwa, S.P. & Jang, J.C. (2014) Tandem CCCH zinc finger proteins in plant growth, development and stress response. *Plant & Cell Physiology*, **55**, 1367–1375.

Eriksson, S., Bohlenius, H., Moritz, T. & Nilsson, O. (2006) GA_4 is the active gibberellin in the regulation of *LEAFY* transcription and *Arabidopsis* floral initiation. *The Plant Cell*, **18**, 2172–2181.

Gu, X., Le, C., Wang, Y., Li, Z., Jiang, D., Wang, Y. *et al.* (2013) Arabidopsis FLC clade members form flowering-repressor complexes coordinating responses to endogenous and environmental cues. *Nature Communications*, **4**, 1947.

Hall, T.A. (1999) BioEdit: a user-friendly biological sequence alignment editor and analysis program for windows 95/98/NT. *Nucleic Acids Symposium Series*, **41**, 95–98.

Harada, H. & Nitsch, J. (1959) Flower induction in Japanese chrysanthemums with gibberellic acid. *Science*, **129**, 777–778.

Hazebroek, J.P., Metzger, J.D. & Mansager, E.R. (1993) Thermoinductive regulation of gibberellin metabolism in *Thlaspi arvense L.* (II. Cold induction of enzymes in gibberellin biosynthesis). *Plant Physiology*, **102**, 547–552.

Hellens, R.P., Allan, A.C., Friel, E.N., Bolitho, K., Grafton, K., Templeton, M.D. *et al.* (2005) Transient expression vectors for functional genomics, quantification of promoter activity and RNA silencing in plants. *Plant Methods*, **1**, 1–14.

Hellens, R.P., Edwards, E.A., Leyland, N.R., Bean, S. & Mullineaux, P.M. (2000) pGreen: a versatile and flexible binary Ti vector for agrobacterium-mediated plant transformation. *Plant Molecular Biology*, **42**, 819–832.

Higuchi, Y., Narumi, T., Oda, A., Nakano, Y., Sumitomo, K., Fukai, S. *et al.* (2013) The gated induction system of a systemic floral inhibitor, antiflorigen, determines obligate short-day flowering in chrysanthemums. *Proceedings of the National Academy of Sciences of the United States of America*, **110**, 17137–17142.

Hisamatsu, T., Koshioka, M. & Mander, L.N. (2004) Regulation of gibberellin biosynthesis and stem elongation by low temperature in Eustoma grandiflorum. *The Journal of Horticultural Science and Biotechnology*, **79**, 354–359.

Hisamatsu, T., Sumitomo, K., Shibata, M. & Koshioka, M. (2017) Seasonal variability in dormancy and flowering competence in chrysanthemum: chilling impacts on shoot extension growth and flowering capacity. *Japan Agricultural Research Quarterly: JARQ*, **51**, 343–350.

Huang, J.C., Ge, X.J. & Sun, M. (2000) Modified CTAB protocol using a silica matrix for isolation of plant genomic DNA. *BioTechniques*, **28**, 432–434.

Huang, P., Chung, M.S., Ju, H.W., Na, H.S., Lee, D.J., Cheong, H.S. *et al.* (2011) Physiological characterization of the *Arabidopsis thaliana* oxidation-related zinc finger 1, a plasma membrane protein involved in oxidative stress. *Journal of Plant Research*, **124**, 699–705.

Huang, P., Ju, H.W., Min, J.H., Zhang, X., Chung, J.S., Cheong, H.S. *et al.* (2012) Molecular and physiological characterization of the *Arabidopsis thaliana* oxidation-related zinc finger 2, a plasma membrane protein involved in ABA and salt stress response through the ABI2-mediated signaling pathway. *Plant & Cell Physiology*, **53**, 193–203.

Jones, P., Binns, D., Chang, H.Y., Fraser, M., Li, W., McAnulla, C. *et al.* (2014) InterProScan 5: genome-scale protein function classification. *Bioinformatics*, **30**, 1236–1240.

Kawata, J. (1987) The phasic development of chrysanthemum as a basis for the regulation of vegetative growth and flowering in Japan. *Acta Horticulturae*, **197**, 280–287.

King, R.W. (2012) Mobile signals in day length-regulated flowering: gibberellins, flowering locus T, and sucrose. *Russian Journal of Plant Physiology*, **59**, 479–490.

Langridge, J. (1957) Effect of day-length and gibberellic acid on the flowering of Arabidopsis. *Nature*, **180**, 36–37.

Lee, D.J. & Zeevaart, J.A. (2007) Regulation of gibberellin 20-oxidase1 expression in spinach by photoperiod. *Planta*, **226**, 35–44.

Lee, S.J., Jung, H.J., Kang, H. & Kim, S.Y. (2012) Arabidopsis zinc finger proteins AtC3H49/AtTZF3 and AtC3H20/AtTZF2 are involved in ABA and JA responses. *Plant & Cell Physiology*, **53**, 673–686.

Lescot, M., Dehais, P., Thijs, G., Marchal, K., Moreau, Y., Van de Peer, Y. *et al.* (2002) PlantCARE, a database of plant cis-acting regulatory elements and a portal to tools for in silico analysis of promoter sequences. *Nucleic Acids Research*, **30**, 325–327.

Lin, P.C., Pomeranz, M.C., Jikumaru, Y., Kang, S.G., Hah, C., Fujioka, S. *et al.* (2011) The Arabidopsis tandem zinc finger protein AtTZF1 affects ABA- and GA-mediated growth, stress and gene expression responses. *The Plant Journal*, **65**, 253–268.

Liu, J., Fan, Y., Zou, J., Fang, Y., Wang, L., Wang, M. *et al.* (2017) A *RhABF2/ferritin* module affects rose (*Rosa hybrida*) petal dehydration tolerance and senescence by modulating iron levels. *The Plant Journal*, **92**, 1157–1169.

Liu, Y.G. & Chen, Y. (2007) High-efficiency thermal asymmetric interlaced PCR for amplification of unknown flanking sequences. *Biotechniques*, **43**, 649–650 652, 654 passim.

Livak, K.J. & Schmittgen, T.D. (2001) Analysis of relative gene expression data using real-time quantitative PCR and the $2^{-\Delta\Delta CT}$ method. *Methods*, **25**, 402–408.

Metzger, J.D. (1985) Role of gibberellins in the environmental control of stem growth in Thlaspi arvense L. *Plant Physiology*, **78**, 8–13.

Michaels, S.D. & Amasino, R.M. (1999) FLOWERING LOCUS C encodes a novel MADS domain protein that acts as a repressor of flowering. *The Plant Cell*, **11**, 949–956.

Mutasa-GÖttgens, E. & Hedden, P. (2009) Gibberellin as a factor in floral regulatory networks. *Journal of Experimental Botany*, **60**, 1979–1989.

Pharis, R.P. (1972) Flowering of chrysanthemum under non-inductive long days by gibberellins and N^6-benzyladenine. *Planta*, **105**, 205–212.

Ratcliffe, O.J., Kumimoto, R.W., Wong, B.J. & Riechmann, J.L. (2003) Analysis of the Arabidopsis MADS AFFECTING FLOWERING gene family: MAF2 prevents vernalization by short periods of cold. *The Plant Cell*, **15**, 1159–1169.

Ream, T.S., Woods, D.P. & Amasino, R.M. (2012) The molecular basis of vernalization in different plant groups. *Cold Spring Harbor Symposia on Quantitative Biology*, **77**, 105–115.

Rieu, I., Ruiz-Rivero, O., Fernandez-Garcia, N., Griffiths, J., Powers, S.J., Gong, F. *et al.* (2008) The gibberellin biosynthetic genes *AtGA20ox1* and *AtGA20ox2* act, partially redundantly, to promote growth and development throughout the Arabidopsis life cycle. *The Plant Journal*, **53**, 488–504.

Saleh, A., Alvarez-Venegas, R. & Avramova, Z. (2008) An efficient chromatin immunoprecipitation (ChIP) protocol for studying histone modifications in Arabidopsis plants. *Nature Protocols*, **3**, 1018–1025.

Schwabe, W.W. (1950) Factors controlling flowering of the chrysanthemum: I. the effects of photoperiod and temporary chilling. *Journal of Experimental Botany*, **1**, 329–343.

Schwabe, W.W. (1954) Factors controlling flowering in the chrysanthemum: IV. The site of vernalization and translocation of the stimulus. *Journal of Experimental Botany*, **5**, 389–400.

Song, Y.H., Ito, S. & Imaizumi, T. (2013) Flowering time regulation: photoperiod- and temperature-sensing in leaves. *Trends in Plant Science*, **18**, 575–583.

Srikanth, A. & Schmid, M. (2011) Regulation of flowering time: all roads lead to Rome. *Cellular and Molecular Life Sciences*, **68**, 2013–2037.

Suge, H. & Rappaport, L. (1968) Role of gibberellins in stem elongation and flowering in radish. *Plant Physiology*, **43**, 1208–1214.

Sumitomo, K., Li, T.P. & Hisamatsu, T. (2009) Gibberellin promotes flowering of chrysanthemum by upregulating *CmFL*, a chrysanthemum *FLORICAULA/LEAFY* homologous gene. *Plant Science*, **176**, 643–649.

Tamura, K., Peterson, D., Peterson, N., Stecher, G., Nei, M. & Kumar, S. (2011) MEGA5: molecular evolutionary genetics analysis using maximum likelihood, evolutionary distance, and maximum parsimony methods. *Molecular Biology and Evolution*, **28**, 2731–2739.

Tang, Y., Wang, F., Zhao, J.P., Xie, K., Hong, Y.G. & Liu, Y.L. (2010) Virus-based microRNA expression for gene functional analysis in plants. *Plant Physiology*, **153**, 632–641.

Thompson, J.D., Higgins, D.G. & Gibson, T.J. (1994) CLUSTAL W: improving the sensitivity of progressive multiple sequence alignment through sequence weighting, position-specific gap penalties and weight matrix choice. *Nucleic Acids Research*, **22**, 4673–4680.

Tilmes, V., Mateos, J.L., Madrid, E., Vincent, C., Severing, E., Carrera, E. *et al.* (2019) Gibberellins act downstream of Arabis PERPETUAL

FLOWERING1 to accelerate floral induction during vernalization. *Plant Physiology*, **180**, 1549–1563.

Vegis, A. (1964) Dormancy in higher plants. *The Annual Review of Plant Biology*, **15**, 185–224.

Wang, R.H., Farrona, S., Vincent, C., Joecker, A., Schoof, H., Turck, F. *et al.* (2009) *PEP1* regulates perennial flowering in *Arabis alpina*. *Nature*, **459**, 423–427.

Wei, Q., Ma, C., Xu, Y., Wang, T., Chen, Y., Lu, J. *et al.* (2017) Control of chrysanthemum flowering through integration with an aging pathway. *Nature Communications*, **8**, 829.

Whittaker, C. & Dean, C. (2017) The *FLC* locus: a platform for discoveries in epigenetics and adaptation. *Annual Review of Cell and Developmental Biology*, **33**, 555–575.

Xu, S. & Chong, K. (2018) Remembering winter through vernalisation. *Nature Plants*, **4**, 997–1009.

Xu, Y.J., Zhao, X., Aiwaili, P., Mu, X.Y., Zhao, M., Zhao, J. *et al.* (2020) A zinc finger protein BBX19 interacts with ABF3 to affect drought tolerance negatively in chrysanthemum. *The Plant Journal*, **103**, 1783–1795.

Yang, Y.J., Ma, C., Xu, Y.J., Wei, Q., Imtiaz, M., Lan, H.B. *et al.* (2014) A zinc finger protein regulates flowering time and abiotic stress tolerance in chrysanthemum by modulating gibberellin biosynthesis. *The Plant Cell*, **26**, 2038–2054.

Zanewich, K.P. & Rood, S.B. (1995) Vernalization and gibberellin physiology of winter canola (endogenous gibberellin (GA)) content and metabolism of [^{3}H] GA_1 and [^{3}H] GA_{20}. *Plant Physiology*, **108**, 615–621.

Zhang, X., Zhou, Y., Ding, L., Wu, Z., Liu, R. & Meyerowitz, E.M. (2013) Transcription repressor HANABA TARANU controls flower development by integrating the actions of multiple hormones, floral organ specification genes, and GATA3 family genes in Arabidopsis. *The Plant Cell*, **25**, 83–101.

Zhong, S., Joung, J.G., Zheng, Y., Chen, Y.R., Liu, B., Shao, Y. *et al.* (2011) High-throughput illumina strand-specific RNA sequencing library preparation. *Cold Spring Harbor Protocols*, **8**, 940–949.